Evaluation of probabilistic constellation shaping performance in Flex-Grid over multi-core fiber dynamic optical backbone networks [Invited]

JORDI PERELLÓ[1,*], JOAN M. GENÉ[1], AND SALVATORE SPADARO[1]

[1] Universitat Politècnica de Catalunya (UPC) - Barcelona Tech, Barcelona, Spain
[*] Corresponding author: jordi.perello@upc.edu

Compiled March 21, 2023

In this paper, we present a worst-case methodology for estimating the attainable spectral efficiency over end-to-end paths across a Flex-Grid over multi-core fiber (MCF) optical network. This methodology accounts for physical link noise, as well as for the signal-to-noise ratio in the Add module (SNR_{TX}) of spatial division multiplexing (SDM)-enabled re-configurable optical add & drop multiplexers (SDM-ROADMs), introducing this one a dominant noise contribution over that of their Bypass and Drop modules. The proposed methodology is subsequently used to quantify the benefits that probabilistic constellation shaping (PCS) can bring to Flex-Grid/MCF dynamic optical backbone networks, compared to using traditional polarization-multiplexed modulation formats. In a first step, insight is provided into the spectral efficiency attainable along the pre-computed end-to-end paths in two reference backbone networks, either using PCS or traditional modulation formats. Moreover, in each one of these networks, two SNR_{TX} values are identified: the SNR_{TX} yielding the maximum average paths' spectral efficiency, as well as an SNR_{TX} that, although slightly degrading average paths' spectral efficiency (by 10%), it would yet enable a cost-effective SDM-ROADM Add module implementation. Extensive simulations are conducted to analyze PCS offered load gains under 1% bandwidth blocking probability (BBP). Furthermore, the study lastly focuses on finding out whether lower fragmentation levels in Flex-Grid/MCF dynamic optical backbone networks can push PCS benefits even further.

http://dx.doi.org/10.1364/ao.XX.XXXXXX

1. INTRODUCTION

Elastic optical networks (EONs) putting Flex-Grid and spatial division multiplexing (SDM) technologies together [1] have emerged as key candidates to implement future optical network infrastructures, taking advantage of their superior flexibility and capacity, reaching far beyond the non-linear Shannon limit of standard single mode fibers (SMFs) [2, 3].

To realize SDM in short-, mid- and long-term optical networks, different candidate technologies have been proposed along the years [4]. In the most straightforward way, SDM can be enabled in the short-term by deploying bundles of SMFs per network link, thus directly scaling the network capacity (i.e., multiplying it by the number of SMFs in these bundles).

However, to be truly beneficial, SDM must also lower the cost and energy per bit of legacy optical transmission systems. And to achieve these goals, appropriate network component integration becomes required, as discussed in [5, 6]. Therefore, mid- and long-term SDM solutions are envisioned to rely on more advanced technological solutions, like multi-core fibers (MCFs), few-mode fibers (FMF) and also few-mode MCFs (FM-MCFs). In MCFs, a single mode is transmitted over each one of the multiple cores cohabiting within the same fiber cladding, while FMFs contain a unique core supporting the transmission of a few modes. FM-MCFs become a combination of the two previous solutions, wherein multiple cores support each one the transmission of a few modes. In particular, high core-count MCFs have already been designed and fabricated to date, showing very low inter-core crosstalk (XT) values with up to 22 and even 30 cores inside the same fiber cladding [7, 8]. Such impressive technological advances advocate for MCFs as a means for introducing SDM in mid- and long-term Flex-Grid optical backbone network infrastructures.

Looking at the literature, countless works on improving the performance of pure Flex-Grid (over SMFs) and also Flex-Grid/SDM optical networks adopt the so-called *distance adaptive spectrum allocation* strategy, initially proposed for the SLICE network in [9]. Other works also name it as *distance adaptive transmission* or *distance adaptive modulation format selection*, being

 DOI 10.1364/JOCN.447423

the same strategy in essence. This strategy consists in selecting the most efficient yet feasible modulation format (MF) for any new lightpath, in view of its maximum transmission reach and the end-to-end transmission distance from the lightpath's source to destination nodes. Traditional polarization-multiplexed (PM) MFs are typically used with this strategy, from PM-BPSK up to advanced PM-*m*-QAM ones (e.g., as in [10–13]).

Nonetheless, probabilistic constellation shaping (PCS) has very recently come to the fore as a technology able to provide a fine-grained software-defined trade-off between achievable spectral efficiency (SE) and transmission distance [14]. Indeed, the wide tunability of PCS has already been demonstrated across the full distance range, from data center interconnects (DCI) to trans-Pacific, using a single 32-GBaud hardware platform [15]. Compared to alternative modulation techniques providing SE fine tuning like geometric constellation shaping (GCS) and time-division hybrid modulation (TDHM), PCS pushes the achievable SE closer to Shannon's Limit [14] and has already shown good results in standard fibers [16]. It becomes therefore noteworthy to investigate the potential benefits stemming from the adoption of PCS in future Flex-Grid/SDM optical networks.

The present paper builds upon and expands the contributions in [17]. There, a worst-case methodology was proposed to estimate the attainable SE along end-to-end paths in a Flex-Grid/MCF optical network, which was employed to shed light into the potential benefits of using PCS versus traditional MFs. Some initial results were extracted in two Flex-Grid/MCF dynamic optical backbone networks. However, these studies did not dig into the effects of node losses on the observed PCS benefits, always setting them equal to 10 dB per intermediate node (Bypass module) along the paths. Furthermore, potential losses occurring at Add/Drop modules of connections' source-destination SDM-ROADMs were neglected in the methodology. Finally, it was left for future work to investigate whether lower spectrum fragmentation levels in Flex-Grid/MCF dynamic optical networks could raise PCS benefits even further.

In light of the above, the key novel contributions of the present expanded paper are summarized as follows:

1. We extend and refine the proposed methodology in [17] to not only account for Bypass losses at SDM-ROADMs, but also for those occurring at their Add/Drop modules. During this process, we identify that, by appropriately designing Bypass modules of SDM-ROADMs, Add module losses become predominant over them and also over those occurring at their Drop modules.

2. We introduce an additional fragmentation-aware route, modulation format, core and spectrum assignment (FA-RMCSA) heuristic, which was not considered in [17]. The motivation behind it is to also evaluate PCS in Flex-Grid/MCF dynamic optical network scenarios with lower spectrum fragmentation levels, thus identifying potential effects of spectrum fragmentation on PCS benefits.

3. We perform a deeper analysis of the attainable SE along the pre-computed paths in the two evaluated reference backbone networks. In particular, we identify two SDM-ROADMs Add module signal-to-noise ratio (SNR_{TX}) values per network. The first of these values yields the maximum attainable SE along the pre-computed paths, while the second would enable a quite realistic Add module implementation at expenses of a slightly degraded paths' SE.

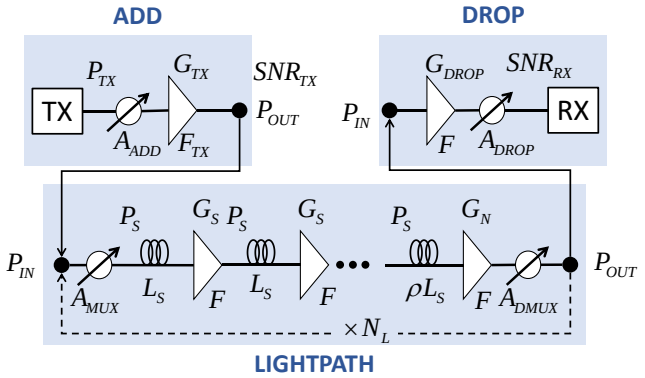

Fig. 1. Lightpath Model. Top-left: Add section. Top-right: Drop section. Bottom: Lightpath section.

4. We conduct new sets of simulations to quantify PCS benefits versus traditional MFs under 1% bandwidth blocking probability (BBP) for each one of the identified SNR_{TX} values in each network. In the conducted simulations, we employ the same RMCSA heuristic as in [17], as well as the fragmentation-aware one newly introduced in this paper.

5. We carefully analyze all obtained results to refine and expand the conclusions already extracted in [17].

The remainder of the paper continues as follows. Section 2 presents the extended path SE estimation methodology. Section 3 introduces the two RMCSA heuristics employed in the conducted simulations. Section 4 presents the obtained numerical results. Finally, Section 5 concludes the paper.

2. LIGHTPATH SPECTRAL EFFICIENCY

The ligthpath model is shown in Fig. 1. It is divided in three parts: the add section, the drop section and the lightpath itself. In the add section, a generic transmitter is defined by its transmission power P_{TX}. The adding mechanism is assumed to introduce an attenuation A_{ADD}, which depends on the underlying architecture. Finally, a booster amplifier is considered with gain G_{TX}, which is responsible for setting the right optical power into the lightpath spans P_S. The dropping mechanism, namely, the adding counterpart, introduces an attenuation A_{DROP}, which is compensated by an optical amplifier with gain G_{DROP}. The lightpath section consists of a number of links N_L that equals the number of intermediate nodes plus one. Each link includes an input multiplexer plus an output demultiplexer with attenuations A_{MUX} and A_{DMUX}, respectively. The link is composed of a number of fiber spans of length L_S, each one with an optical amplifier with gain G_S to compensate for the span losses. The last span to complete the link is typically a fraction $\rho \leq 1$ of L_S and needs to be treated separately. The last amplifier corresponds to the node's front amplifier, whose gain G_N compensates for the last span losses plus the attenuation introduced by the signal's demultiplexing and multiplexing. Compensating for node losses using the front amplifiers makes the optical signal-to-noise ratio (OSNR) to be independent of them. This is reasonable when the required gain does not exceed 40 dB, which limits node losses for bypass traffic to 23 dB (maximum span losses are 17 dB, see details below).

The OSNR at the receiver SNR_{RX} can be decomposed into 2 factors: the OSNR at the channel's input SNR_{TX} and the OSNR

due to the channel alone, SNR_C, which corresponds to SNR_{RX} when SNR_{TX} equals infinity (noiseless transmitter).

$$\frac{1}{SNR_{RX}} = \frac{1}{SNR_{TX}} + \frac{1}{SNR_C} \quad (1)$$

The first term is independent of the span's input power P_S and reads:

$$SNR_{TX} = \underbrace{\frac{P_{TX}}{hf \cdot F_{TX} R_S}}_{SNR_0} A_{ADD} \quad (2)$$

where h is Planck's constant, f is the optical frequency, F_{TX} is the amplifier's noise factor, and R_S is the symbol rate. SNR_0 is defined as the OSNR for a lossless adding architecture. On the other hand, the channel's OSNR can be maximized by choosing the optimum signal's input power P_S [18], which balances out the amplified spontaneous emission (ASE) noise and the nonlinear interference noise (NLIN). A full link transparency is assumed forcing the span input power to be constant along the lightpath. Even though this is a sub-optimum situation (i.e., every span should be optimized independently), all spans are assumed to be uniform except the last ones before reaching the node, which leaves a very small margin for improvement. This, together with the simplicity of the method, justifies the assumption. SNR_C then reads [18]:

$$SNR_C = \frac{1}{3\left[\chi P_{ASE}^2 / 4\right]^{1/3} + \kappa \cdot L} \quad (3)$$

where P_{ASE} corresponds to ASE noise power within the channel's bandwidth at the receiver. As shown in Fig.1, lumped amplification is assumed with 85-km spans and attenuation parameter $\alpha = 0.2\, dB/km$. The amplifier's noise figure is assumed to be $F = 5\, dB$ in all cases. χ is the equivalent NLIN parameter assuming the *Gaussian Noise Model* [19]. To calculate it, a nonlinear parameter $\gamma = 1.3\ W^{-1}km^{-1}$ is assumed, together with a dispersion parameter $D = 17\ ps \cdot nm^{-1}km^{-1}$. Also, a fully loaded C-band $B_W = 4\ THz$ is considered, which corresponds to the worst-case. Aggregate XT experienced by a core from signals co-propagating at the same wavelength in all other cores simultaneously is captured by parameter κ (accumulated XT per unit distance) multiplied by the lightpath length L. When all cores are active, the maximum XT level is generated, which again corresponds to the worst-case scenario. An optimized MCF layout is assumed, which provides the same κ for all cores. As shown in [20], there exists an optimum XT level of about -55 dB/km that maximizes the aggregate capacity. This corresponds to an optimum number of cores for each MCF outer diameter. This value is taken as a reference in our calculations assuming an optimized 22-core MCF which corresponds to a moderate 250-micron cladding diameter (twice the current standard). Ideal Nyquist pulse shaping is assumed which is seen as realistic given current state-of-the art technology. Provided that all spans are considered uniform, the calculation of the end-to-end χ is essentially the nonlinear parameter of a single span χ_S multiplied by the number of whole spans N_S in the path composed by N_L links [19]. The last span in every internodal link needs to be treated separately, as its length is a fraction ρ_i of a regular span and the gain of the corresponding amplifier must be reduced accordingly. The following formula is obtained:

$$\chi = \chi_S \left(N_S + \sum_{i=1}^{N_L} \left\{ 1 - G_S^{-\rho_i} \right\}^2 \right) \quad (4)$$

where [19]:

$$\chi_S = \frac{16}{27}\gamma^2 \frac{c}{\lambda^2 |D| R_S^2} \frac{10^4}{\alpha \ln 10} asinh\left(\frac{\pi}{4} \frac{\lambda^2 |D| B_W^2}{c} \frac{10^4}{\alpha \ln 10} \right) \quad (5)$$

Fractional spans require special treatment when calculating P_{ASE} as well. The overall expression reads:

$$P_{ASE} = h \cdot f \left\{ \left(G_S N_S + \sum_{i=1}^{N_L} G_S^{\rho_i} \right) + A_{MUX} \right\} F \cdot R_S \quad (6)$$

A_{MUX} term comes from the drop amplifier in Fig. 1. Notice that the product χP_{ASE}^2 is symbol rate independent, which makes SNR_C symbol rate independent as well.

The maximum SE (b/s/Hz) per polarization-multiplexed spatial path using an adaptive modulation such as PCS and ideal Nyquist pulse shaping is given by [20]:

$$SE = 2 \cdot log_2 \left(1 + \frac{1}{\frac{1}{SNR_{TX}} + 3\left[\chi P_{ASE}^2 / 4\right]^{1/3} + \kappa \cdot L} \right) \quad (7)$$

The suggested procedure provides the worst-case SE calculation. This value can be pre-computed only once (i.e., offline), thus simplifying resource management. The busier the network it gets, the more accurate the calculations become. In other words, the spectrum assignment becomes more efficient when spectral efficiency is most required.

3. RMCSA HEURISTICS

The most appropriate route, modulation format, core and spectrum portion must be decided when allocating each incoming lightpath in a Flex-Grid/MCF dynamic optical network. For this purpose, two RMCSA heuristics are proposed in this work, called RMCSA-first fit (RMCSA-FF) and fragmentation aware-RMCSA (FA-RMCSA). It is worth mentioning that these RMCSA heuristics do not contemplate the existence of any lightpath regeneration capability in the network (i.e., we assume a completely transparent Flex-Grid/MCF optical network). Furthermore, they also exclude any possibility to split the required spectrum for a lightpath into multiple portions/blocks for their separate allocation in the same or different MCF cores (inverse multiplexing is not considered in this work).

A. Offline path pre-computation

Both RMCSA-FF and FA-RMCSA heuristics assume an offline path pre-computation, where the k shortest physical paths (in km) between every source-destination node pair in the network are initially pre-computed, using the well-known Yen's algorithm [21]. Moreover, the attainable SE over each pre-computed physical path is subsequently obtained using the previously proposed methodology in section 2.

Two different situations are contemplated here, depending on whether PCS or traditional MFs are employed in the network. In the first situation (PCS employed in the network), the SE value of each pre-computed physical path is directly equal to the value obtained using the proposed methodology. In contrast, in the second situation (traditional MFs used in the network), the most efficient MF offering a SE value lower or equal to the resulting one from the methodology is selected for each path. For example, imagine that the proposed methodology estimates an attainable SE value equal to 9.25 b/s/Hz over a specific physical path. When using PCS, the SE of that path becomes directly

equal to this value. Conversely, when using traditional MFs (e.g., PM-BPSK, PM-QPSK, PM-16-QAM, PM-64-QAM and PM-256-QAM), PM-16-QAM is selected, hence the SE of that path becomes equal to 8 b/s/Hz.

Algorithm 1 describes the offline path pre-computation, where $G(N, E)$ represents the Flex-Grid/MCF network graph, with N and E being the sets of network nodes and links, respectively. Moreover, M denotes the set of candidate traditional MFs (used in certain situations to benchmark PCS performance), with m_{SE} being the SE of any $m \in M$. Finally, P denotes the set of all pre-computed physical candidate paths in the network. That is, if (s, d) represents any pair of source-destination nodes and P_{sd} the set of pre-computed candidate physical paths between them, then $P = \cup_{s \in N, d \in N, s \neq d} P_{sd}$. For any path $p \in P$, the attainable SE over it is represented as p_{SE}.

Algorithm 1. Offline path pre-computation

```
1:  procedure OFFLINEPATHPRECOMPUTATION(G, M, k)
2:      for s ∈ N do
3:          for d ∈ N do
4:              if s ≠ d then
5:                  P_sd ← KShortestPaths(G, s, d, k)
6:                  P ← P ∪ P_sd
7:      for p ∈ P do
8:          SE ← proposedMethodology(p)
9:          if PCS used in network then
10:             p_SE ← SE
11:         else
12:             p_SE ← m_SE      ▷ Most eff. m ∈ M with m_SE ≤ SE
13:     return P
```

B. RMCSA-FF heuristic

This heuristic (Algorithm 2) is the one that was used to obtain the results in previous work [17]. To describe it, imagine an incoming demand request of B Gb/s between source-destination node pair (s, d). RMCSA-FF explores its possible allocation over a spectral super-channel on any $p \in P_{sd}$, starting from the shortest to the longest one, on a first-fit fashion. To this end, the required number of frequency slots (FS) for allocating the super-channel over path p is obtained as $n_{FS} = \lceil (B/p_{SE} + \Delta)/W \rceil$, where Δ denotes the imposed guard-band width between adjacent spectral super-channels in the network and W the FS width, both expressed in GHz. Note that, although no guard-bands were assumed in the methodology proposed in section 2, RMCSA-FF accounts for them as an additional safety margin.

Next, an available spectral portion of n_{FS} contiguous and continuous FSs is sought in any core along the currently explored candidate path, also on a first-fit fashion. We assume in Algorithm 2 that MCF links comprise C cores (indexed by $c_i \in \{1, ..., C\}$), offering each one S FSs in total (indexed by $s_i \in \{1, ..., S\}$). If such a spectrum portion is found, the demand request is considered served using these resources. However, if no available spectrum portion is found along any core of any $p \in P_{sd}$, the demand request is considered as blocked eventually.

C. FA-RMCSA heuristic

The second FA-RMCSA heuristic (Algorithm 3) has been newly introduced in this paper to investigate whether lower spectrum fragmentation levels can boost PCS benefits, which was left open for future work in [17].

Algorithm 2. RMCSA-FF heuristic

```
1:  procedure RMCSA-FF(G, P, B, s, d)
2:      P_sd ← getPathsOrderedByIncreasingDistance(P, s, d)
3:      for p ∈ P_sd do
4:          n_FS = ⌈(B/p_SE + Δ)/W⌉
5:          for c_i = 1 to C do
6:              for s_i = n_FS to S do
7:                  if allSlotsFree(G, p, c_i, s_i − n_FS + 1, s_i) then
8:                      allocateAllSlots(G, p, c_i, s_i − n_FS + 1, s_i)
9:                      return Served
10:     return Blocked
```

To describe its operation, imagine again an incoming demand request of B Gb/s between source-destination node pair (s, d). Like the previous heuristic, FA-RMCSA tries to allocate the new demand over a spectral super-channel on any $p \in P_{sd}$, starting from the shortest to the longest one. To this goal, for each path, it firstly computes the required n_{FS} value. Then, it starts exploring the available cores along the path (indexed again as $c_i \in \{1, ..., C\}$), looking for an available spectral gap with a width exactly equal to n_{FS} to allocate the spectral super-channel, on a first-fit manner. If this spectral gap is found, the demand request is served using these resources.

Conversely, if no available spectral gap of exactly n_{FS} FSs is found on any core along that path, FA-RMCSA tries to allocate it again on the same cores of the same path. In this case, it seeks for the largest available spectral gap in every core, denoted as Θ. If the gap found is wider or equal to n_{FS} FSs (we assume it of width equal to 0 when not found), the demand request is served using these resources. Please note in Algorithm 3 that we denote as $\Theta_{s_{ini}}$ the initial FS of Θ. Conversely, if no appropriate gap is found in any core, the next path $p \in P_{sd}$ is explored, following exactly the same actions as detailed before. If no appropriate gap is found along any core of any $p \in P_{sd}$, the demand request is finally considered as blocked.

Algorithm 3. FA-RMCSA heuristic

```
1:  procedure FA-RMCSA(G, P, B, s, d)
2:      P_sd ← getPathsOrderedByIncreasingDistance(P, s, d)
3:      for p ∈ P_sd do
4:          n_FS = ⌈(B/p_SE + Δ)/W⌉
5:          for c_i = 1 to C do
6:              for s_i = n_FS to S do
7:                  if isExactGap(G, p, c_i, s_i − n_FS + 1, s_i) then
8:                      allocateAllSlots(G, p, c_i, s_i − n_FS + 1, s_i)
9:                      return Served
10:         for c_i = 1 to C do
11:             Θ ← findLargestGap(p, c_i)
12:             if spectralWidth(Θ) ≥ n_FS then
13:                 allocateAllSlots(G, p, c, Θs_ini, Θs_ini + n_FS − 1)
14:                 return Served
15:     return Blocked
```

As a matter of fact, the spectrum assignment performed by FA-RMCSA is quite similar to the *exact-fit* policy proposed for pure Flex-Grid over SMF networks in [22], which was shown to effectively lower network spectrum fragmentation levels. In light of this, we have slightly extended such a strategy for the purposes of this work, making it also applicable to Flex-Grid/MCF networks.

Finally, note that RMCSA-FF and FA-RMCSA enforce core

continuity end-to-end. This decision has been motivated by the potential deployment of cost-effective SDM-ROADMs without lane-change support, which deliver similar performance to fully-flexible independent switching (InS) ones in dynamic Flex-Grid/MCF networks, as evaluated in [13].

D. Algorithmic complexity

The proposed offline path pre-computation procedure runs a number of $|N|(|N|-1)$ times the Yen's algorithm [21] to obtain the k shortest physical paths between every source-destination node pair. Yen's algorithm has a well-known computational complexity of $\mathcal{O}(k|N|(|E|+|N|\log|N|))$. Then, for each one of the $|P|$ pre-computed paths, the proposed methodology is executed to obtain its attainable SE value. Since the methodology needs to check all links traversed by a path to obtain the output SE value, the computational complexity of this part can be upper bounded by $\approx \mathcal{O}(|P||E|)$. So, the overall computational complexity of the offline path pre-computation can be upper bounded by $\approx \mathcal{O}(k|N|^3(|E|+|N|\log|N|)+|P||E|)$.

Regarding RMCSA-FF, it firstly sorts the pre-computed paths between source-destination node pair (s,d), being k paths at most. By using an efficient sorting algorithm, the computational complexity of this step can be upper bounded by $\mathcal{O}(k\log k)$. Next, it explores all cores along the sorted paths to find an available contiguous spectral portion of the required number of FSs. And when found, FSs must be reserved afterwards. Such operations are most demanding when the required number of FSs is equal to $S/2$. So, this part of the heuristic can be upper bounded by $\mathcal{O}(kC(S/2+1)S/2+S/2) \approx \mathcal{O}(kCS^2/4)$. The overall computational complexity of RMCSA-FF can therefore be upper bounded by $\approx \mathcal{O}(k\log k + kCS^2/4))$.

As for FA-RMCSA, a similar analysis can be performed. The computational complexity of sorting the pre-computed paths between (s,d) can be bounded by $\mathcal{O}(k\log k)$. Then, for each sorted path, FA-RMCSA explores all cores aiming to find a gap of width exactly equal to the required number of FSs, which can be upper bounded by $\approx \mathcal{O}(CS^2/4)$. If not found, all cores are explored again seeking for the largest available gap on them and, when sufficiently large, the required FSs are allocated. We can bound the complexity of this part as $\approx \mathcal{O}(CS)$. Finally, the overall FA-RMCSA computational complexity can be upper bounded by $\approx \mathcal{O}(k\log k + k(CS^2/4+CS))$.

For illustrative purposes, note that in backbone networks as the considered ones in this work (see section 4.A), we measure average RMCSA-FF and FA-RMCSA execution times around 2 and 4 ms, respectively, with k values up to 6. Regarding the offline path pre-computation, it also runs quite fast given the worst-case nature of the proposed methodology. With k values up to 6, for example, the complete offline path pre-computation takes less than 150 ms in the considered backbone networks. Such execution times have been extracted in a standard Intel Core i3 9^{th} Gen computer equipped with 8 GB RAM.

4. NUMERICAL RESULTS

This section presents the numerical results obtained in this work using an ad-hoc Python-based simulator. We firstly present all details of the considered evaluation scenarios and the assumptions taken. Secondly, we perform a deep analysis of the characteristics of the offline pre-computed candidate paths. Thirdly, we simulate the considered Flex-Grid/MCF dynamic optical backbone networks and compare the performance of PCS against that of using traditional MFs, employing the previously proposed RMCSA-FF heuristic. Finally, we execute additional simulations employing the alternative FA-RMCSA heuristic in order to reproduce network scenarios with lower spectrum fragmentation, also assessing PCS performance on them.

A. Scenario details and assumptions

Two reference backbone networks have been considered in this work, namely, the national Deutsche Telekom network DT12 (with 12 nodes, 20 bidirectional links and average link length equal to 243 km) and the Pan-European EON16 network (with 16 nodes, 23 bidirectional links and average link length equal to 486 km). The interested reader can find additional details about them in [13]. We assume both networks equipped with SDM-ROADMs without lane change support and 22-core MCF links, which corresponds to a well-proven MCF core-count technology. Moreover, we assume the entire 4 THz C-Band available in all MCF cores, discretized into 320 FSs of 12.5 GHz width.

During network operation (as in the experiments reported in subsection 4.C), we assume that demand requests arrive at the network following a Poisson traffic process, describing exponentially distributed inter-arrival and holding times, with mean values equal to IAT and HT, respectively. To generate different loads, we fix $IAT = 1.0$ and scale HT accordingly (offered load = HT/IAT). When a new demand request arrives, we consider it of 400, 800 or 1200 Gb/s with probability 0.4, 0.4 or 0.2, respectively. Incoming demand requests should be allocated over spectral super-channels, adding $\Delta = 10$ GHz guard-bands between adjacent ones. This value has been chosen based on the specifications of cutting-edge WaveShaper programmable optical filters, providing a bandwidth setting resolution of 1 GHz and a bandwidth setting accuracy of 5 GHz [23].

As for the traditional MFs employed to benchmark PCS performance benefits in our experiments (hereafter referred to as TrMFs), we contemplate PM-BPSK, PM-QPSK, PM-16-QAM, PM-64-QAM and PM-256-QAM, with offered SE values of 2, 4, 8, 12 and 16 b/s/Hz, respectively. Note that we limit the studies to QAM modulations describing square-like constellations, being the simplest and most commonly used ones.

B. Analysis of pre-computed paths

Before starting to offer dynamic traffic to DT12 and EON16 networks, the set of candidate paths between all source-destination node pairs in them is pre-computed offline, as detailed in subsection 3.A. These candidate paths are the ones used later on by the proposed RMCSA-FF and FA-RMCSA heuristics, so as to properly allocate the spectral super-channels carrying the incoming dynamic demand requests.

In order to give insight into the characteristics of pre-computed paths in DT12 and EON16 networks, Fig. 2 shows their average SE (in b/s/Hz) as a function of SNR_{TX} when using PCS or TrMFs, assuming k values equal to 1, 3 and 6. Looking at the figure, we can realize that average path SE values always decrease with k. This is very reasonable, as higher k values lead to pre-computing longer paths, which accumulate more noise that negatively impacts their SE end-to-end. Moreover, SNR_{TX} also plays a key role on paths' average SE, particularly when falling below 30 dB in the DT12 and 24 dB in the EON16, that is, when noise generated within the Add module of source SDM-ROADMs starts being noticeable.

In the same Fig. 2, it is noteworthy the coarser granularity of TrMFs. When using them in the DT12 (Fig. 2, top), it can be appreciated that paths employ PM-64-QAM and PM-16-QAM with

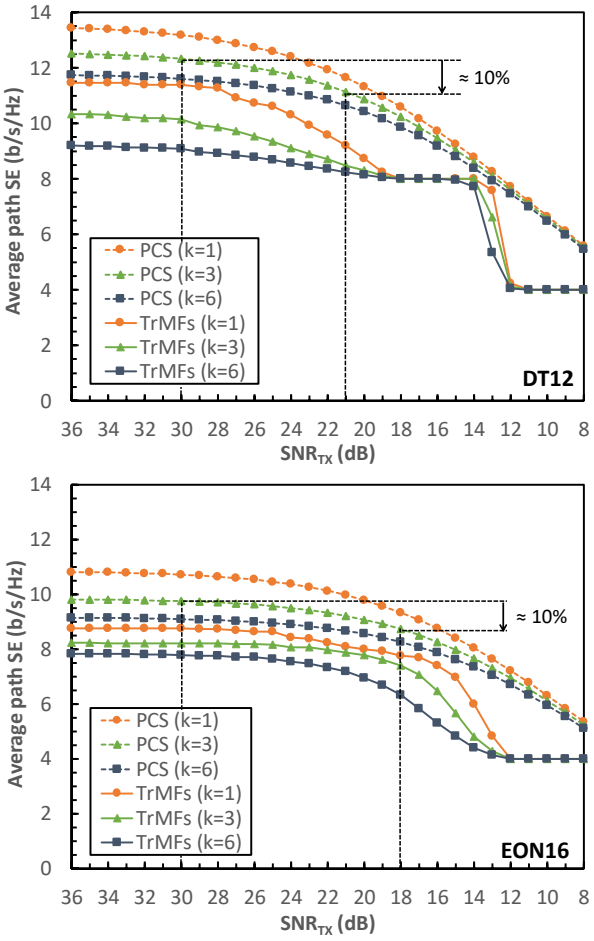

Fig. 2. Average SE value of pre-computed paths in the DT12 (top) and EON16 (bottom) networks vs. SNR_{TX}.

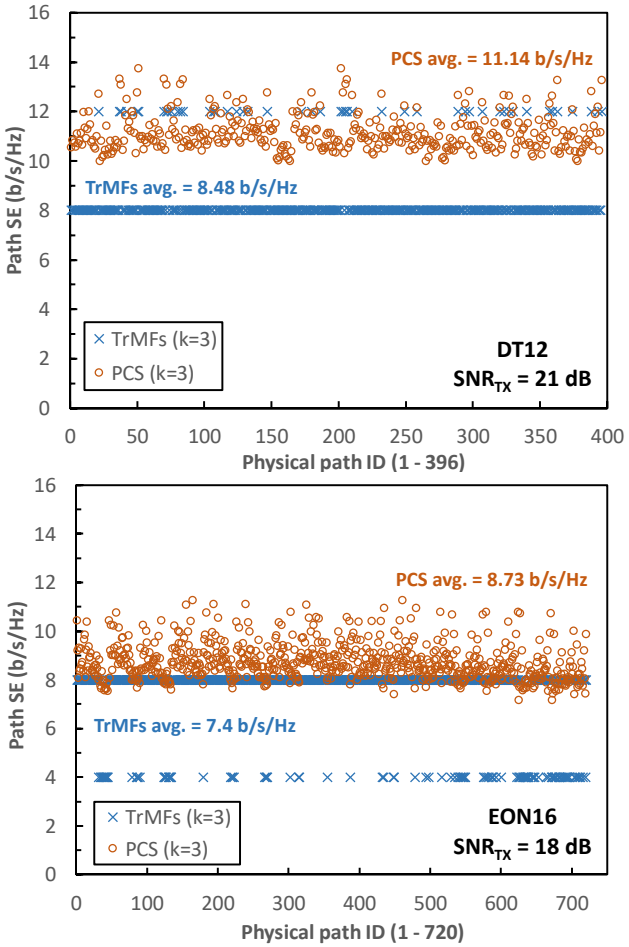

Fig. 3. Individual pre-computed path SE in the DT12 with SNR_{TX} = 21 dB (top) and EON16 with SNR_{TX} = 18 dB (bottom), when using PCS or TrMFs (k = 3 in all cases).

high SNR_{TX} values (i.e., avg. paths' SE values lie in between 8-12 b/s/Hz). However, as SNR_{TX} decreases, all paths tend to use PM-16-QAM (avg. paths' SE = 8 b/s/Hz) and then PM-QPSK (avg. paths' SE = 4 b/s/Hz). It is particularly abrupt the jump from 8 down to 4 b/s/Hz at SNR_{TX} = 14 dB, indicating that most paths suddenly need to change from using PM-16-QAM to PM-QPSK when lowering SNR_{TX} even further.

In the EON16 (Fig. 2, bottom), longer distances exist between source-destination node pairs. Therefore, when using TrMFs, most paths start using PM-16-QAM, even with high SNR_{TX} (avg. paths' SE values only slightly higher than 8 b/s/Hz). Then, as SNR_{TX} decreases, every time more paths require PM-QPSK. In contrast, these steps are not observed at all when PCS is employed, showing a gentle average paths' SE reduction vs. SNR_{TX}, thanks to its finer granularity. Furthermore, PCS always yields better outcomes.

High SNR_{TX} is thus key for maximizing paths' SE, no matter if PCS or TrMFs are employed in the network. However, from an implementation perspective, highly complex and expensive devices with very low losses might be required in the Add module of SDM-ROADMs to achieve such a high SNR_{TX}. Hence, alternative cost-effective solutions might be convenient. To also contemplate them, we firstly select in DT12 and EON16 networks SNR_{TX} = 30 dB as a value (almost) maximizing average paths' SE. Moreover, we also select in each network an alternative SNR_{TX} value that, although slightly degrading paths' SE (by 10%, we assume), it would ease the implementation of the Add module in SDM-ROADMs. We have focused on PCS curves with k = 3 to decide these alternative values, namely, 21 and 18 dB in the DT12 and EON16 networks. Assuming a realistic SNR_0 = 40 dB, such SNR_{TX} values would allow employing 64 and 128 splitting ratios to implement the Add module of SDM-ROADMs, respectively, in contrast to those limited to 8 required for an SNR_{TX} = 30 dB. Large splitting allows for transceiver sharing, which translates into cost reduction [24].

In particular, in the DT12 with k = 3 and SNR_{TX} = 30 dB, TrMFs achieve average paths' SE equal to 10.14 b/s/Hz, which raises up to 12.33 b/s/Hz when PCS is employed (21.6% higher). In the EON16 with the same k and SNR_{TX} values, TrMFs yield average paths' SE equal to 8.22 b/s/Hz, also outperformed by PCS (9.76 b/s/Hz, 18.73% higher). As for the selected cost-effective SNR_{TX} values, in the DT12 with k = 3 and SNR_{TX} = 21 dB, TrMFs and PCS deliver average paths' SE equal to 8.48 and 11.14 b/s/Hz (31% higher). And in the EON16 with k = 3 and SNR_{TX} = 18 dB, TrMFs and PCS achieve 7.4 and 8.73 b/s/Hz (i.e., 18% higher), respectively. These last results become particularly interesting, highlighting that relative PCS benefits versus TrMFs do not seem to be affected at all when adopting cost-effective SDM-ROADM Add module implementations. In fact, they even grow up in the DT12 (from 21.6 up to 31%).

Individual path SE values behind the measured averages are

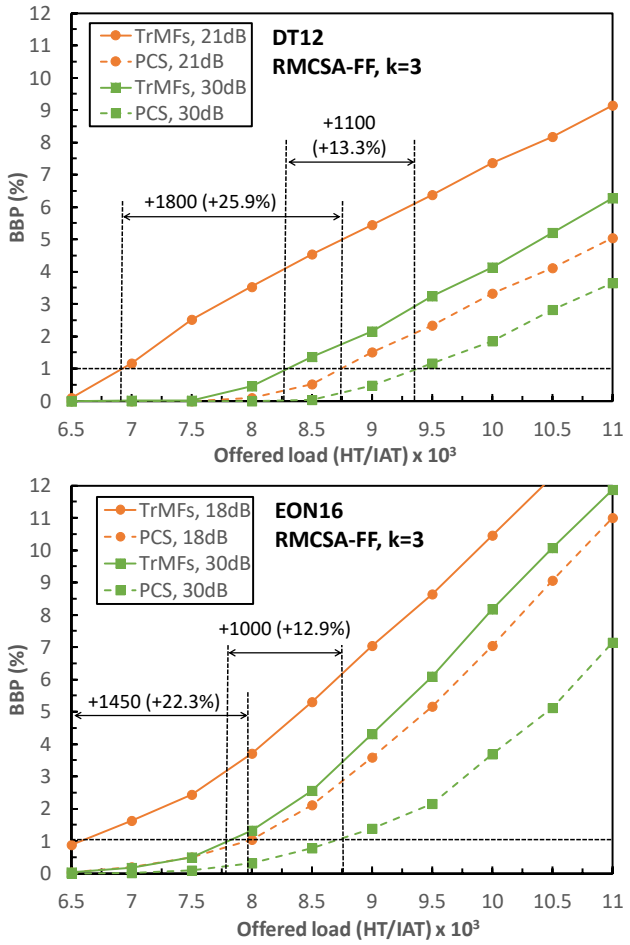

Fig. 4. Average BBP versus offered load in the DT12 (top) and EON16 (bottom) networks when RMCSA-FF (k = 3).

also illustrated in Fig. 3 for DT12 (top) and EON16 (bottom) networks. SNR_{TX} equal to 21 and 18 dB in DT12 and EON16 are taken as examples. Moreover, k = 3 has also been selected, resulting in the pre-computation of 396 (i.e., 12*11*3) paths in the DT12, and 720 (i.e., 16*15*3) paths in the EON16. As seen, the vast majority of paths in the DT12 with TrMFs employ PM-16-QAM, while only a few can employ PM-64-QAM. Conversely, all paths show SE values ranging from 10-14 b/s/Hz with PCS, approximately. In the EON16 with TrMFs, many paths end using PM-16-QAM and sometimes even PM-QPSK, while path SE values with PCS range from 7-11 b/s/Hz. The depicted average values are the ones described in the paragraph above.

C. Dynamic network scenarios

At this point, we start offering dynamic demand requests and quantify the experienced BBP on both networks. Please note that $k = 3$ has been always set in this subsection when pre-computing paths in both networks, a typical value considered in most related works in the literature.

Fig. 4 depicts the measured BBP in the DT12 (top) and EON16 (bottom) networks as a function of the offered load, when employing PCS or TrMFs on them. Two different SNR_{TX} values have been assumed in each network, namely, the one maximizing paths' average SE (i.e., 30 dB) and the cost-effective one selected in previous subsection (21 dB in the DT12 and 18 dB in the EON16). 250k demand requests have been offered per execution. Moreover, all included results in this figure have been obtained using the RMCSA-FF heuristic.

As observed in the DT12 network (Fig. 4, top), employing PCS results in significantly reduced network BBP against TrMFs. With SNR_{TX} = 30 dB, the superior behavior of PCS allows offering an additional load of 1100 units to the network (relative offered load increment of 13.3%), while keeping BBP = 1%, a reference BBP value that we identify as an operational network scenario. The relative benefits of using PCS further increase when lowering SNR_{TX} down to 21 dB. Indeed, while TrMFs rapidly reach BBP = 1%, PCS allows offering 1800 more load units to the network under the same BBP value (relative increment of 25.9%). In the EON16 (Fig. 4, bottom), similar outcomes are observed, as PCS allows offering an additional 1000 load units (12.9% increment) compared to TrMFs under BBP = 1% with SNR_{TX} = 30 dB. And such differences increase up to 1450 additional load units (22.3% offered load increment) when lowering SNR_{TX} down to 18 dB. Therefore, although relative PCS benefits in terms of average paths' SE remained similar in the EON16 when assuming SNR_{TX} = 18 dB (recall the results in previous subsection), PCS ends up providing higher admissible offered load relative gains versus TrMFs, which can serve as a motivation toward cost-effective SDM-ROADM designs.

In fact, the observed results with SNR_{TX} = 30 dB in DT12 and EON16 networks are very similar to those obtained in previous work [17]. Besides assuming identical backbone networks, traffic profile and RMCSA heuristic, this can be explained as follows. In [17], intermediate node losses equal to 10 dB were assumed to obtain the end-to-end SE of the pre-computed paths, while losses at SDM-ROADM Add/Drop modules were neglected. Such intermediate node losses may have impaired OSNR, but 10 dB were still unnoticeable. Indeed, SNR_{TX} = 30 dB yields a similar result, being significantly higher than SNR_C.

Finally, we aim to investigate whether PCS benefits become limited by the spectrum fragmentation in Flex-Grid/MCF dynamic optical networks and can raise using a fragmentation-aware RMCSA heuristic, which was left for future work in [17]. To this goal, we firstly validate the FA-RMCSA heuristic proposed in subsection 3.C to ensure that it effectively reduces network spectrum fragmentation. To do that, we measure the spectrum external fragmentation (F_{ext}) metric [22], which can be formulated as $F_{ext} = 1 - FSsLargestAvailableGap/TotalAvailableFSs$. F_{ext} tends to 0 (or 1) when the size in FSs of the largest available gap becomes similar to (or very small compared to) the total number of available FSs, detecting no (or high) fragmentation of the spectrum.

In our experiments, we measure F_{ext} in the following way. Every 10k offered demand requests (i.e., 25 times along the complete simulations with 250k offered requests), we measure F_{ext} for every pre-computed path and core along them. Specifically, we get the spectrum occupancy of cores along each pre-computed path by overlapping the spectrum occupancy of that core in all traversed MCFs. That is, a FS is considered available when it becomes available in that core in all MCFs along the path. Otherwise, being a FS occupied in that core in at least one traversed MCF, it is directly considered as so. Once having F_{ext} measures for every pre-computed path and core, we average them afterwards to obtain a single F_{ext} metric value.

Table 1 illustrates some F_{ext} values measured in both DT12 (denoted as N1 due to table space limitations) and EON16 (N2) networks when setting SNR_{TX} = 30 dB and using RMCSA-FF. Besides, Table 2 shows the same results, but employing FA-RMCSA instead. Comparing both tables, FA-RMCSA effectively

Table 1. Average F_{ext} with RMCSA-FF (SNR_{TX} = 30 dB)

Load	TrMFs (N1)	PCS (N1)	TrMFs (N2)	PCS (N2)
7000	0.55	0.499	0.583	0.625
8000	0.606	0.56	0.568	0.617
9000	0.615	0.612	0.549	0.608
10000	0.614	0.623	0.54	0.596

Table 2. Average F_{ext} with FA-RMCSA (SNR_{TX} = 30 dB)

Load	TrMFs (N1)	PCS (N1)	TrMFs (N2)	PCS (N2)
7000	0.418	0.391	0.402	0.475
8000	0.457	0.423	0.384	0.452
9000	0.464	0.472	0.371	0.433
10000	0.464	0.48	0.357	0.415

reduces F_{ext} in all cases. We have checked that FA-RMCSA also achieves similar F_{ext} reduction for all offered load and SNR_{TX} evaluated scenarios in DT12 and EON16 networks. Therefore, we can safely use it for evaluating PCS behavior under lower spectrum fragmentation.

Fig. 5 shows the average BBP in both DT12 (top) and EON16 (bottom) networks as a function of the offered network load, when using PCS or TrMFs. The same SNR_{TX} values as in previous Fig. 4 have been considered. However, results have now been obtained using the FA-RMCSA heuristic with $k = 3$, offering again 250k demand requests per execution.

Looking at Fig. 5, slightly lower BBP values than those previously depicted in Fig. 4 can be observed, which demonstrates the better resource allocation decisions of FA-RMCSA, compared to those of the simpler RMCSA-FF. Indeed, PCS benefits from the better allocation decisions, but also TrMFs. So, differences increase in some cases (e.g., in the DT12 with SNR_{TX} = 21 dB, from 1800 to 1950 load units), but in others they decrease (e.g., in the EON16 with SNR_{TX} = 30 dB, from 1000 to 800 load units). In any case, employing PCS with cost-effective SDM-ROADM implementations still provides very significant relative benefits in terms of admissible offered load (above 20-25%), which should pay the Digital Signal Processing (DSP) complexity needed for its eventual realization.

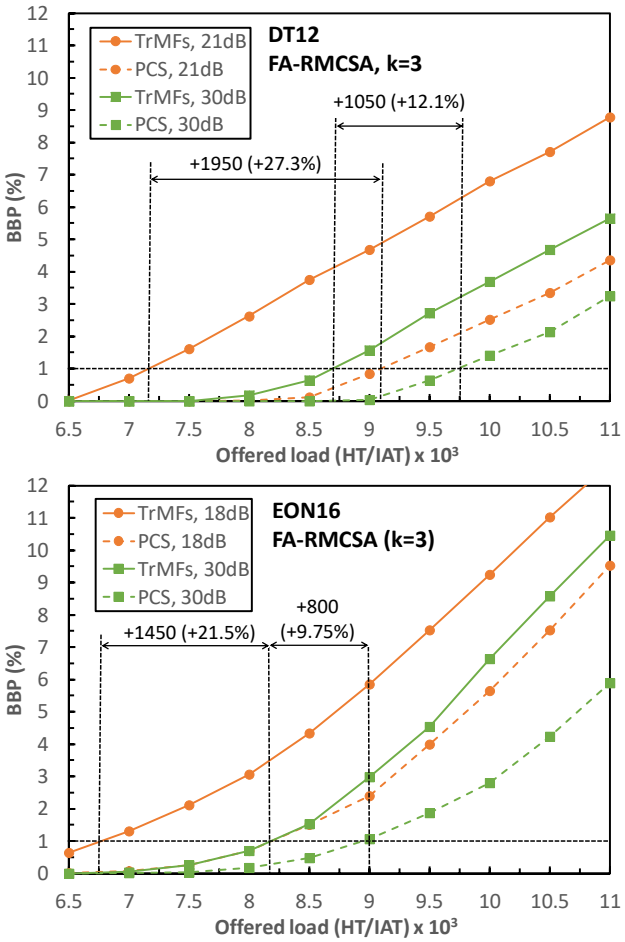

Fig. 5. Average BBP versus offered load in the DT12 (top) and EON16 (bottom) networks using FA-RMCSA (k = 3).

5. CONCLUSIONS AND FUTURE WORK

This paper proposes a worst-case methodology for estimating the attainable SE along pre-computed paths in Flex-Grid/MCF optical networks, not only accounting for Bypass losses at SDM-ROADMs, but also for those at their Add/Drop modules. Once identified SDM-ROADM Add module losses as dominant, the proposed methodology is employed to evaluate PCS against traditional polarization-multiplexed modulation formats in Flex-Grid/MCF dynamic optical backbone networks. Two RMCSA heuristics are proposed, a first-fit (RMCSA-FF) and a fragmentation-aware one (FA-RMCSA). Numerical results are extracted in two reference backbone networks, analyzing the attainable SE along the pre-computed paths. This allows identifying specific SDM-ROADM Add module signal-to-noise ratio (SNR_{TX}) values, either maximizing paths' SE or slightly degrading them but enabling cost-effective implementations. Dynamic network scenarios are also evaluated, being PCS performance clearly superior. It is remarkable that relative PCS gains increase in cost-effective SDM-ROADM designs. All in all, we can safely advocate for PCS as a strong candidate for realizing future Flex-Grid/MCF dynamic optical backbone networks.

As a future work, authors plan to employ quality of transmission (QoT) models able to estimate lightpaths XT levels taking into account the actual neighboring cores spectrum occupancy in traversed MCFs. Focus will be put on evaluating whether the required additional computational complexity (versus the worst-case XT level assumption taken in this work) pays off in terms of additional carried network load, particularly in low and moderate network load scenarios.

FUNDING

Spanish State Research Agency (AEI): PID2020-118011GB-C21, PID2020-118011GB-C22, RED2018-102585-T.

ACKNOWLEDGMENTS

This publication is part of the Spanish I+D+i projects TRAINER-A and TRAINER-B (refs. PID2020-118011GB-C21 and PID2020-118011GB-C22), funded by MCIN/AEI/10.13039/501100011033. Moreover, it has been supported by the Spanish Thematic Network under contract RED2018-102585-T (Go2Edge).

Portions of this work were presented at the International Conference on Optical Network Design and Modelling (ONDM) 2021, in the paper entitled *On the Benefits of Probabilistic Constellation Shaping in Flex-Grid/MCF Dynamic Optical Backbone Networks*.

REFERENCES

1. D. Klonidis, F. Cugini, O. Gerstel, M. Jinno, V. Lopez, E. Palkopoulou, M. Sekiya, D. Siracusa, G. Thouénon, and C. Betoule, "Spectrally and spatially flexible optical network planning and operations," IEEE Commun. Mag. **53**, 69–78 (2015).
2. A. Chralyvy, "Plenary paper: The coming capacity crunch," in European Conference on Optical Communication (ECOC) 2009 (2009).
3. P. J. Winzer, "Spatial Multiplexing: The Next Frontier in Network Capacity Scaling," in European Conference and Exhibition on Optical Communication (ECOC) 2013, paper We.1.D.1 (2013).
4. G. M. Saridis, D. Alexandropoulos, G. Zervas, and D. Simeonidou, "Survey and evaluation of space division multiplexing: From technologies to optical networks," IEEE Commun. Surv. & Tutorials **17**, 2136–2156 (2015).
5. P. J. Winzer, "Making spatial multiplexing a reality," Nat. Photonics **8**, 345–348 (2014).
6. P. J. Winzer, and D. T. Neilson, "From Scaling Disparities to Integrated Parallelism: A Decathlon for a Decade," J. Light. Technol. **35**, 1099–1115 (2017).
7. B. J. Puttnam, R. S. Luís, W. Klaus, J. Sakaguchi, J.-M. Delgado Mendinueta, Y. Awaji, N. Wada, Y. Tamura, T. Hayashi, M. Hirano, and J. Marciante, "2.15 Pb/s transmission using a 22 core homogeneous single-mode multi-core fiber and wideband optical comb," in European Conference on Optical Communication (ECOC) 2015, paper PDP.3.1 (2015).
8. Y. Amma, Y. Sasaki, K. Takenaga, S. Matsuo, J. Tu, K. Saitoh, M. Koshiba, T. Morioka, and Y. Miyamoto, "High-density Multicore Fiber with Heterogeneous Core Arrangement," in Optical Fiber Communication Conference (OFC) 2015, paper Th4C.4 (2015).
9. M. Jinno, B. Kozicki, H. Takara, A. Watanabe, Y. Sone, T. Tanaka, and A. Hirano, "Distance-Adaptive Spectrum Resource Allocation in Spectrum-Sliced Elastic Optical Path Network," IEEE Commun. Mag. **48**, 138–145 (2010).
10. R. Goscien, K. Walkowiak, and M. Klinkowski, "Distance-Adaptive Transmission in Cloud-Ready Elastic Optical Networks," J. Opt. Commun. Netw. **6**, 816–828 (2014).
11. P. Khodashenas, J. Rivas-Moscoso, D. Siracusa, F. Pederzolli, B. Shariati, D. Klonidis, E. Salvadori, and I. Tomkos, "Comparison of Spectral and Spatial Super-Channel Allocation Schemes for SDM Networks," J. Light. Technol. **34**, 2710–2716 (2016).
12. J. Perelló, J. M. Gené, A. Pagès, J. A. Lazaro, and S. Spadaro, "Flex-Grid/SDM Backbone Network Design with Inter-Core XT-limited Transmission Reach," J. Opt. Commun. Netw. **8**, 540–552 (2016).
13. R. Rumipamba-Zambrano, F.-J. Moreno-Muro, J. Perelló, P. Pavón-Mariño, and S. Spadaro, "Space continuity constraint in dynamic flex-grid/SDM optical core networks: An evaluation with spatial and spectral super-channels," Computer Communications **126**, 38–49 (2018).
14. J. Cho, and P. J. Winzer, "Probabilistic Constellation Shaping for Optical Fiber Communications," J. Light. Technol. **37**, 1590–1607 (2019).
15. J. M. Gené, X. Chen, J. Cho, S. Chandrasekhar, and P. J. Winzer, "Experimental Demonstration of Widely Tunable Rate/Reach Adaptation From 80 km to 12,000 km Using Probabilistic Constellation Shaping," in Optical Fiber Communication Conference (OFC) 2020, paper M3G.3 (2020).
16. O. Karandin, F. Musumeci, O. Ayoub, A. Ferrari, Y. Pointurier and M. Tornatore, "Quantifying Resource Savings from Low-Margin Design in Optical Networks with Probabilistic Constellation Shaping," in European Conference on Optical Communication (ECOC) 2021, 1–4 (2021).
17. J. Perelló, J. M. Gené, and S. Spadaro, "On the Benefits of Probabilistic Constellation Shaping in Flex-Grid/MCF Dynamic Optical Backbone Networks," in International Conference on Optical Network Design and Modelling (ONDM) 2021, 1–3 (2021).
18. T. Hayashi, T. Taru, O. Shimakawa, T. Sasaki, and E. Sasaoka, "Uncoupled multi-core fiber enhancing signal-to-noise ratio," Opt. Express, **20**, B94–B103 (2012).
19. P. Poggiolini G. Bosco, A. Carena, V. Curri, Y. Jiang, and F. Forghieri, "The GN-model of fiber non-linear propagation and its applications," J. Light. Technol. **32**, 694–721 (2014).
20. J. M. Gené, P. Winzer, H. Chen, R. Ryf, T. Hayashi, and T. Sasaki, "Towards broadly optimum multi-core fiber designs," in European Conference and Exhibition on Optical Communication (ECOC) 2019, 1–4 (2019).
21. J. Y. Yen, "Finding the K Shortest Loopless Paths in a Network," Management Science **17**, 712–716 (1971).
22. A. Rosa, C. Cavdar, S. Carvalho, J. Costa, and L. Wosinska, "Spectrum Allocation Policy Modeling for Elastic Optical Networks," in International Symposium on High Capacity Optical Networks and Enabling Technologies (HOTNET) 2012, 242–246 (2012).
23. II-VI Incorporated. Optical Instrumentation (2022, January 19th). https://ii-vi.com/product-category/products/optical-communications/optical-instrumentation/
24. D. M. Marom, P. D. Colbourne, A. D'Errico, N. K. Fontaine, Y. Ikuma, R. Proietti, L. Zong, J. M. Rivas-Moscoso, and I. Tomkos, "Survey of photonic switching architectures and technologies in support of spatially and spectrally flexible optical networking [invited]," J. Opt. Commun. Netw. **9**, 1–26 (2017).